

# Withdrawing the Edge-Read Permission of Graph Convolutional Network to Against Adversarial Attack

Ao Liu, Beibei Li, and Tao Li

**Abstract**—Node classification based on graph convolutional networks (GCNs) is vulnerable to adversarial attacks by malicious perturbations on graph structures, such as inserting or deleting graph edges. In this paper, by given a general attack model, we concretize the vulnerability of the GCN into a concrete description: The *edge-read permission* to GCN makes it vulnerable. We propose the Anonymous GCN (AN-GCN) which capable of making nodes participate in classification anonymously, thus withdraw the *edge-read permission* of the GCN. Extensive evaluations demonstrate that, by keeping the anonymity of node position while classification, AN-GCN block malicious perturbations passing along to the visible edge, meanwhile keep high accuracy (2.93% higher than the state of the art GCN)

**Index Terms**—Adversarial Attack, Graph Convolutional Network, General Attack Model, Anonymous Classification.



## 1 INTRODUCTION

Graph is the core for many high impact applications ranging from the analysis of social networks, over gene interaction networks, to interlinked document collections. In many tasks related to the graph structure, node classification, predicting labels of unknown nodes based on a small number of labeled known nodes, is always a hot issue.

However, vulnerabilities of predicting the node category have been gradually explored. Only slight deliberate perturbations of nodes' features or graph structure can lead to completely wrong predictions. That is, GCNs suffer from poor adversarial robustness – they are sensitive to small adversarial perturbations designed to achieve a malicious goal. Take for example a GNN-based model for detecting fake news on a social network [1] [2]. Adversaries have a strong incentive to fool the system in order to avoid detection. In this context, a perturbation could mean modification of the graph structure (inserting or deleting edges in the social graph). Even in scenarios where adversaries are unlikely, understanding the robustness of GNNs to worst-case noise is important, especially in safety-critical applications.

Message passing driven by end-to-end training is the core operation powering modern GCNs. In the message passing steps, the embedding of the node is updated by aggregating over its neighbors' embeddings, which will lead to a self-contradictory problem: on the one hand, the message passing on the graph ensures efficient and accurate node prediction, on the other hand, it facilitates the global passing of malicious perturbations, which lead to the fact that a well-designed malicious perturbation will unavoidably pass to the target node. The aforementioned contradictory problem can be the vulnerability of GCN.

To address the vulnerability of GCN, we present an improved GCN model, which capable of classifying the node

according to its features without its position, thus blocking malicious perturbations passing to the specific target node.

In this work, we transform the vulnerability of GCN into a solvable concrete problem. Specifically, we re-examine the encoding and decoding process of GCN, give a *general attack model* against GCN, and further come to a concrete conclusion: The GCN will be vulnerable if it directly takes edges as input.

Therefore, we propose the Anonymous GCN (AN-GCN) to withdraw the *edge-read permission* of the model. In AN-GCN, the position of nodes will be generated from the noise randomly, while ensuring the high-accuracy classification, that is, nodes are classified while keeping *anonymous* to their position. Since the edge decides the node position, the anonymity of the position eliminates the necessity of edge-reading for AN-GCN, thus solving the vulnerability of GCN.

We first figure out how GCN deconstructs the initial input to keep the node fixed in its position during training, thus transform the node location method of GCN to a computable mathematical expression. Specifically, by regarding the feature change of each node in the training process as the independent signal vibration, we map the signal vibrations of all nodes to the Fourier domain with a unified coordinate system, finally build the *Node signal model* to directly emerge how GCN locate nodes.

According to the given mathematical expression of the node location, we directly generate the node position by a generator (designed as a fully connected network) to replace the corresponding part in GCN. For ensuring generation effective, we improve the pioneering spectral GCN [3] to a discriminator, which trying to detect nodes with the generated position. Because the discriminator is a self-contained GCN, it will classify the node with generative position accurately once the above two-player game well played.

Our main contributions include:

- Ao Liu, Beibei Li, and Tao Li are with School of Cyber Science and Engineering, Sichuan University.

- We propose a *general attack model* against GCN, which proves that the edge-read permission to GCN makes it vulnerable.
- We build a node signal model to represent the node signal vibration in the training process, according to the model, we give the mathematical expression for the method of the GCN locating node.
- We present a technique for generating node positions from noise, while ensuring high-accuracy classification, so as to solve the vulnerability of GCN

The rest of the paper is organized as follows. In Sec. 3, the GCN training process is re-examined from the perspective of encoding and decoding. The vulnerability of GCN is concretized as the edge-read permission. In Sec. 4.1, by establishing the node signal model, the signal vibration equation of the node is given, which is used to analyze how the model locates the nodes in the GCN training process. In Sec. 4.3 and Sec. 4.4, we describe the structure of the proposed AN-GCN, including the generator, discriminator, and training methods. In Sec. 5, we comprehensively evaluated the theoretical results and models proposed in this paper, includes the effectiveness of our proposed general attack model, the effectiveness of the claimed node localization method, the classification accuracy of AN-GCN, in addition, the robustness of AN-GCN to the adversarial samples.

## 2 RELATED WORK

**Graph Attacks Against GCNs.** In 2018, Dai *et al.* [4] and Zügner *et al.* [5] first proposed adversarial attacks on graph structures, after which a large number of graph attack methods were proposed. Specific to the task of node prediction, Chang *et al.* [6] attacked various kinds of graph embedding models with black-box driven, Aleksandar *et al.* [7] provided the first adversarial vulnerability analysis on the widely used family of methods based on random walks, derive efficient adversarial perturbations that poison the network structure. Wang *et al.* [8] proposed a threat model to characterize the attack surface of a collective classification method, targeting adversarial collective classification. Basically, all attack types are based on the perturbed graph structure targeted by this article.

**Defenses for GCNs without GAN.** Tang *et al.* [9] investigated a novel problem of improving the robustness of GNNs against poisoning attacks by exploring a clean graph and created supervised knowledge to train the ability to detect adversarial edges so that the robustness of GNNs is elevated. Jin *et al.* [10] used the new operator in replacement of the classical Laplacian to construct an architecture with improved spectral robustness, expressivity, and interpretability. Zügner *et al.* [11] proposed the first method for certifiable (non-)robustness of graph convolutional networks with respect to perturbations of the node attributes. Zhu *et al.* [12] proposed RGCN to automatically absorb the effects of adversarial changes in the variances of the Gaussian distributions.

**Defenses for GCNs with GAN.** Some defense methods also use adversarial training to enhance the robustness of the model. Deng *et al.* [13] presented batch virtual adversarial training (BVAT), a novel regularization method for graph convolutional networks (GCNs). By feeding the

model with perturbing embeddings, the robustness of the model is enhanced by them. But this method trains a full-stack robust model for the encoder and decoder at the same time, without discussing the essence of the vulnerability of GCN. Wang *et al.* [14] investigated latent vulnerabilities in every layer of GNNs and proposed corresponding strategies including dual-stage aggregation and bottleneck perceptron. Then, to cope with the scarcity of training data, they proposed an adversarial contrastive learning method to train GNN in a conditional GAN manner by leveraging high-level graph representation. But from a certain point of view, they still used the method based on node perturbation for adversarial training. This method is essentially a kind of "perturbation" learning and uses adversarial training to adapt the model to various custom perturbations. Feng [15] proposed Graph Adversarial Training (GAD), which takes the impact from connected examples into account when learning to construct and resist perturbations, introduces adversarial attack on the standard classification to the graph.

## 3 THE VULNERABILITY OF GCN

In this section, we give a general attack model by re-examining the detailed process of graph convolution, and proved that the vulnerability of the graph is caused by the exposure of graph nodes. Specifically, in Sec. 3.1, we divide the training process of GCN into encoding and decoding, and give the mathematical expression formula to support the attack model. In Sec. 3.2, we give the general attack model. In Sec. 3.3, according to the proposed general attack model, we give the concrete description of GCN vulnerability.

### 3.1 Graph convolution encoding and decoding

Let  $\mathcal{G} = (f, \mathcal{E})$  be a graph, where  $f = (f(1), \dots, f(N))^T$  is set of features of  $N$  nodes, while  $f(i)$  is the feature vector of node  $i$ , and  $\mathcal{E}$  is the set of edges which further decide positions of all node. The adjacent matrix  $A \in \mathbb{R}^{N \times N}$  and degree matrix  $D \in \mathbb{R}^{N \times N}$  can be calculated according  $\mathcal{E}$ . According to  $D$  and  $A$ , the laplacian matrix  $\Delta$  of  $\mathcal{G}$  can be obtained. The one-hot code of all node categories on  $\mathcal{G}$  is  $\mathcal{V}$ . Since  $A$  is calculated by  $\mathcal{E}$ , so the graph structure (simultaneously, node positions) can be represented by  $A$ . The process of graph convolution training model on labeled graph dataset is as follows:

**Encoding.** Encode is a node feature aggregation [16] process according to  $\mathcal{E}$ . The graph convolution model maps  $f$  into the embedding space  $f^e = (f^e(1), \dots, f^e(N))^T$  through trainable parameter  $\theta^E$ , while  $f^e(i)$  denotes the embedding feature vector of node  $i$ . Let ENC denotes encoder, the encode process is denoted as:

$$f^e = \text{ENC}(f; A, \theta^E), \quad (1)$$

encode can represent the discrete graph structure into a continuous embedded space [17], which can learn to represent graph nodes, edges or subgraphs in low-dimensional vectors [18]. Many studies [19], [20], [21], [22] visualized the encoded graph to evaluate the effectiveness of model

**Decoding.** Then model decodes  $f^e$  to the one-hot label space  $\mathcal{L} \sim \mathbb{R}^{l \times 1}$  through the decoder DEC (In general,

it is GCN layers) with the trainable parameter  $\theta^D$ ,  $\iota$  is the number of categories. The output of the decoder provides gradient descent direction for GCN model training (usually, the distinction between encoder and decoder is flexible, for example, in multi-layer GCN, the first few layers can be regarded as encoders, and the remaining layers can be regarded as decoders). Almost all high performance Graph Neural Networks models (GraphSAGE [23], GAT [24], spectral-GCN [25], et al.) set the encoder and decoder to the same-design layer, that is, both encoding and decoding involve the aggregation of graph structures  $\mathcal{E}$ , so the decoder parameters still contain  $\mathcal{E}$ . The decoding process is denoted as:

$$\mathcal{Y} = \text{DEC} \left( f^E; \mathbf{A}, \theta^E \right), \quad (2)$$

the decoder calculates output according to  $\mathbf{A}$  and  $f^E$ .

**Training.** According to the labeled nodes, the parameters of encoder and decoder are trained from end-to-end to complete the accurate node prediction task. In the training process, we can add regularization  $\text{Reg}(\cdot)$  (*l1 - norm* [26], et al.) to improve the generalization ability of the model. the training process can expressed as:

$$\arg \min_{\theta^G} \sum \left\{ \text{Loss} \left[ \mathcal{Y}, \text{DEC}(\text{ENC}(f; \mathbf{A}, \theta^E); \mathbf{A}, \theta^D) \right] + \text{Reg}(\theta^G) \right\}, \quad (3)$$

where  $\text{Loss}$  is loss function and  $\theta^G$  is the total parameter set, that is,  $\theta^E$  and  $\theta^D$ . Eq. 3 is the unified form of current graph convolution training methods, and it is computationally universal (Graph neural networks with sufficient parameters are always computationally universal [27]).

### 3.2 General attack model

Given a target graph  $\mathcal{G}_T$  and the target GCN well-trained on  $\mathcal{G}_T$  with the parameter  $\theta_T^G$ , the graph attack perturbs the graph connection, and make classification of the target node changed by traversing the perturbations on  $\mathcal{G}_T$  to obtain  $\mathcal{G}_{victim} = (f, \mathcal{E}_{victim})$ . The attack is to find a modified graph adjacency matrix  $\hat{\mathbf{A}}$  corresponding  $\mathcal{E}_{victim}$ , let

$$\hat{\mathcal{Y}}_\kappa = \text{GCN} \left( f; \hat{\mathbf{A}}, \theta_T^G \right), \quad (4)$$

where  $\kappa$  denotes the node of modified category,  $\hat{\mathcal{Y}}_\kappa$  denotes the distribution of modified node category set in  $\mathcal{L}$ . That is, in  $\hat{\mathcal{Y}}_\kappa$ , the category of  $\kappa$  is manipulated as the target category meanwhile categories of other nodes keep original categories (include single-target and multi-target). From the perspective of model optimization objective [28], it could be either evasion [29], [30] attack or poisoning attack [31], [32], [33]. Once  $\hat{\mathbf{A}}$  is found,  $\mathcal{E}_{victim}$  can be calculated by  $\hat{\mathbf{A}}$ , further effectively attack. We conclude the attack as a  $\hat{\mathbf{A}}$ -finding game:

$$\hat{\mathbf{A}} = \text{ATTACK} \left( \theta_T^E, \theta_T^D, \mathcal{E} \right), \quad (5)$$

where  $\theta_T^E$  and  $\theta_T^D$  is the parameter of the encoder and decoder of the target GCN. In other words, the attacker perturb  $\theta_T^E$ ,  $\theta_T^D$  and  $\mathcal{E}$ , thus find  $\hat{\mathbf{A}}$  to complete the attack. Next we will prove that by manipulating  $\mathcal{E}$ , the attacker

can completely control  $\theta_T^E$  and  $\theta_T^D$ , to further concretize the attack.

Eq. 4 can be expressed as:

$$\hat{\mathcal{Y}}_\kappa = \underset{\text{surrogate}}{\text{DEC}} \left[ \underset{\text{surrogate}}{\text{ENC}} \left( f; \hat{\mathbf{A}}, \theta_T^E \right); \hat{\mathbf{A}}, \theta_T^D \right], \quad (6)$$

once the attacker successfully obtains  $\hat{\mathbf{A}}$  in Eq. 6, the attack will be completed, furthermore, it takes advantage of the vulnerability of GCN. Next, connect target node  $\kappa$  to a *complete graph*  $\bar{\mathcal{G}}$  which each node has closed loops, the diagonal matrix and adjacency matrix of  $\bar{\mathcal{G}}$  are  $\bar{\mathbf{D}}$  and  $\bar{\mathbf{A}}$  respectively, The node feature sets of  $\bar{\mathcal{G}}$  and  $\mathcal{G}$  are same, and the node category set of  $\bar{\mathcal{G}}$  is  $\hat{\mathcal{Y}}_\kappa$ . In order to find  $\hat{\mathbf{A}}$  in Eq. (6), the attack can conclude as following step:

- Introduce a *surrogate* GCN which has the same layer structure and parameters with the target GCN, in the *surrogate* GCN,  $\theta_T^E$  and  $\theta_T^D$  is frozen.
- Set a trainable parameter matrix  $\mathcal{H}$  to *surrogate* GCN.
- Take  $\bar{\mathcal{G}}$  as the input of *surrogate* GCN.
- **Forward propagation.** In training epoches,  $\hat{\mathbf{A}}$  is dynamic changed decided by  $\mathcal{H}$ . Specifically, let  $\mathcal{H} + \mathcal{H}^\top$  act on  $\bar{\mathbf{A}}$  by Hadamard Product, other calculation methods remain unchanged with target GCN.
- **Back propagation.** Calculate the loss of the output and  $\hat{\mathcal{Y}}_\kappa$ , and update  $\mathcal{H}$  according to the loss. (remind that  $\theta_T^E$  and  $\theta_T^D$  is frozen.)

The schematic illustration of the attack is shown as Fig 1.

In this process, Hadamard product makes trainable matrix modify  $\bar{\mathbf{A}}$  element by element, and let  $\mathcal{H}$  plus  $\mathcal{H}^\top$  is to ensure the symmetry of the modified matrix. Let  $\mathcal{H}' = \mathcal{H} + \mathcal{H}^\top$ , the adjacency matrix of graph after attack  $\hat{\mathbf{A}} = \mathcal{H}' \odot \bar{\mathbf{A}}$ , where  $\odot$  represents Hadamard Product. Since  $\bar{\mathbf{A}}$  is a matrix in which all elements are 1 ( $\bar{\mathcal{G}}$  is a full connection graph with closed loop), so  $\hat{\mathbf{A}} = \mathcal{H}'$ . Therefore the solution of  $\bar{\mathbf{D}}$  and  $\bar{\mathbf{A}}$  in Eq. (6) is transformed into the solution of  $\mathcal{H}'$ :

$$\hat{\mathcal{Y}}_\kappa = \underset{\text{surrogate}}{\text{DEC}} \left[ \underset{\text{surrogate}}{\text{ENC}} \left( f; \mathcal{H}', \theta_T^E \right); \mathcal{H}', \theta_T^D \right], \quad (7)$$

where  $\underset{\text{surrogate}}{\text{ENC}}$  and  $\underset{\text{surrogate}}{\text{DEC}}$  is the encoder and decoder of the surrogate GCN, respectively.

Next, considering that the attacker will not perturb the connection directly connected with  $\kappa$  for concealment, so  $\mathcal{H}'$  no longer perturbs line  $\kappa$  of  $\mathbf{A}$ , so  $\mathcal{H}'$  in Eq. (7) is replaced with  $\mathcal{H}'_\kappa = (\mathcal{H}'_1, \dots, \mathbf{A}_\kappa, \dots, \mathcal{H}'_N)^\top$ , where  $\mathcal{H}'_i$  denotes the  $i$ -th row of  $\mathcal{H}'$ . Furthermore, in order to obtain concealed perturbs, attackers need to minimize the amount of perturbation. Specifically, it can be reduced by adding regularization  $\text{Reg}(\mathcal{H}'_\kappa) = \text{Sum}(\mathbf{A} - \mathcal{H}'_\kappa \odot \bar{\mathbf{A}})$  where  $\text{Sum}$  denotes the sum of all elements of matrix (used to indicate the total degree of perturbation). Therefore, the attacker can complete the attack by finding  $\mathcal{H}'_\kappa$ , it can be obtained according to Eq. (8).

$$\arg \min_{\mathcal{H}'_\kappa} \sum \left\{ \text{Loss} \left[ \hat{\mathcal{Y}}_\kappa, \underset{\text{surrogate}}{\text{DEC}} \left( \underset{\text{surrogate}}{\text{ENC}} \left( f; \mathcal{H}'_\kappa, \theta_T^E \right); \mathcal{H}'_\kappa, \theta_T^D \right) \right] + \text{Reg}(\mathcal{H}'_\kappa) \right\}. \quad (8)$$

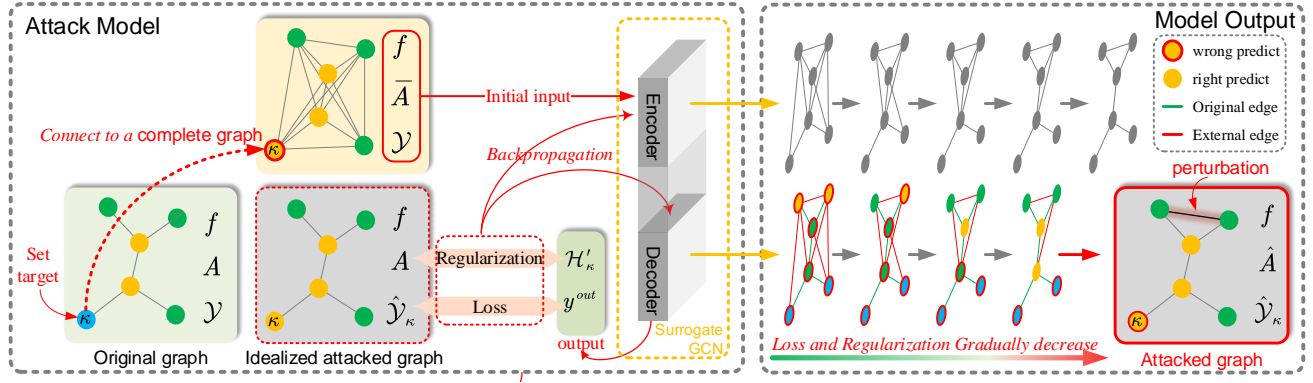


Fig. 1. Attack model

As can be seen, Eq. (8) and Eq. (3) are essentially the same, since Eq. (3) is the unified training method of GCN and Eq. (8) is computationally universal, so, if the attacker wants to modify the node category set, it can be realized by another GCN training task. Since Eq. (4) is the general mathematical formula for attacks and Eq. (8) is derived from Eq. (4), so we conclude that attacker can control  $\theta_{\mathcal{T}}^E$  and  $\theta_{\mathcal{T}}^D$  by manipulating  $\mathcal{E}$ .

In Sec. 5, we will evaluate the performance of Eq. (8) by implementing the attack.

### 3.3 Regard the vulnerability of the GCN as Edge-read permission

By manipulating  $\mathcal{E}$  to control the encoder and decoder, Eq. (5) becomes:

$$\hat{A} = \underset{essence}{\text{ATTACK}}(\mathcal{E}). \quad (9)$$

Eq. (9) shows the essence of the attack target is the exposed graph structure, that is, the specific location of the node. As long as the GCN model directly receives the graph structure as the input, the feasible perturbation can be found through Eq. (8) to realize the attack. In other words, the vulnerability of the GCN caused by the edge-read permission.

### 3.4 Case study

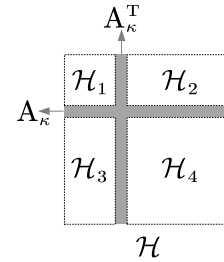
In this section, we describe in detail how to obtain attack methods by training another GCN. Specifically, using semi-GCN [25] as the specific encoding and decoding method to get  $\mathcal{G}_{victim}$ , expressed as Eq. (10):

$$\arg \min_{\mathcal{H}'_{\kappa}} \sum \left\{ \text{Loss} \left[ \hat{\mathcal{Y}}_{\kappa}, \text{Softmax}(\mathcal{H}'_{\kappa} \text{Relu}(\mathcal{H}'_{\kappa} f W_1) W_2) \right] + \text{Reg}(\mathcal{H}'_{\kappa}) \right\}. \quad (10)$$

where  $W_1$  and  $W_2$  well-trained parameter of target GCN. Next, we introduce the details of the experiment. we consider two scenarios: Single target, and multiple targets.

#### 3.4.1 Single target

**Trainable parameter matrix.** In order to ensure  $\mathcal{H}'_{\kappa} = (\mathcal{H}'_1, \dots, A_{\kappa}, \dots, \mathcal{H}'_N)^{\top}$ , we set the trainable parameters  $\mathcal{H}$  to 4 sub matrices:  $\mathcal{H}_1 \in \mathbb{R}^{(\kappa-1) \times (\kappa-1)}$ ,  $\mathcal{H}_2 \in \mathbb{R}^{(\kappa-1) \times (N-\kappa)}$ ,

Fig. 2. Trainable parameter matrix  $\mathcal{H}$  under single node attack

$\mathcal{H}_3 \in \mathbb{R}^{(N-\kappa) \times (\kappa-1)}$ ,  $\mathcal{H}_4 \in \mathbb{R}^{(N-\kappa) \times (N-\kappa)}$ , and they are placed in  $\mathcal{H}$  as shown in the figure 2.

**Layer weight constraint.** In order to make the modified  $\hat{A}$  only have two elements: 0 and 1, we set up layer weight constraints term:

$$\mathcal{H}_{i,j} = \begin{cases} 0 & \text{s.t. } A_{i,j} \geq O_{i,j} \\ 1 & \text{s.t. } A_{i,j} < O_{i,j} \end{cases} \quad (11)$$

where  $\mathcal{H}_{i,j}$  denotes the element in  $\mathcal{H}$  with indices as  $i, j$ ,  $O$  denotes parameters before layer weight constraint.

**Layer weight initializer.** Each trainable sub matrices in  $\mathcal{H}$  is initialize as elements which same as the corresponding indices of  $A$ :

$$\mathcal{H}_{i,j}^{(0)} = A_{i,j}^{(0)} \quad (12)$$

#### 3.4.2 Multiple targets

In the case of multiple targets, let  $\mathcal{K} = \{\kappa_1, \dots, \kappa_N\}$  denote target node set.

**Trainable parameter matrix.** The model flexibility of multi-target attack will be limited by setting too many sub matrices, so all the elements of  $\mathcal{H}$  can be trained, and ensuring the concealment of attacks in regularizer.

**Regularizer.** To minimize the number of direct perturbations to the target node, we need to minimize the number of modifications to the  $\kappa$ -th row of  $\hat{A}$ . The regularizer for multi-target attack is designed as:

$$\text{Sum} \left( A - \mathcal{H}'_{\kappa} \odot \bar{A} \right) + \vartheta \sum_{\kappa \in \mathcal{K}} \text{Sum} (h_{\kappa}), \quad (13)$$

where  $h_{\kappa}$  denotes the  $\kappa$ -th row of  $\mathcal{H}$ ,  $\vartheta$  denotes custom coefficient.

## 4 AN-GCN: KEEP NODE CLASSIFICATION ACCURATE AND ANONYMOUS

In Sec. 3, the vulnerability of GCN is concretized as the edge-read permission of GCN. In this section, we will withdraw the edge read permission of GCN. We integrate a generator and a self-contained GCN to ensure that all node positions are generated from the noise, to ensure that the classification only according to the node index and feature, thus make GCN no longer rely on the information of the edge for classification.

### 4.1 How GCNs locate nodes

The messages are constantly passing while the GCN training, which also can regard as a kind of signal transmission, meanwhile, the feature of the node are constantly changing, we regard it as an independent signal vibration.

In this section, we will build a mathematical model of the node signal vibration to figure out how GCN analyzes the given graph structure to locate nodes. In Sec. 4.1.2, the basic mathematical model for node signal is given. In Sec. 4.1.3, the node signal in the Fourier domain in GCN is described, which process includes two parts: 1. The initial position of the node signal in the Fourier domain is given by blocking the transmission of graph signal; 2. The model of node signal change in the GCN process is given by the introduction of trainable parameters of signal transmission on graphs. Specifically, we first regard the change of each node feature as the signal changing with time (in training, it's the form of epoch)  $t$ , and then map all the node signals to the same orthogonal basis through Fourier transform. Furthermore, we give the node signal model in GCN training, which is used to find the method of GCN locating specific nodes. The method of building the node signal model is shown in the Fig 3.

*Notation.* Let  $\mathcal{G} = (f, \mathcal{E})$  be a graph, where  $f$  is set of features of  $N$  nodes, while  $f(i)$  is the feature of node  $i$  and  $\mathcal{E}$  denotes the set of edges. An essential operator in spectral graph analysis is the graph Laplacian, which combinatorial definition is  $\Delta = D - A$  where  $D \sim \mathbb{R}^{N \times N}$  is the degree matrix and  $A \sim \mathbb{R}^{N \times N}$  is the adjacent matrix (Both  $D$  and  $A$  can be calculated from  $\mathcal{E}$ ). Set the Laplacian matrix of  $\mathcal{G}$  is  $\Delta$  which eigenvalue are  $\lambda_1, \dots, \lambda_N$ , and the corresponding

eigen matrix of  $\Delta$  is  $U = \begin{pmatrix} u_1(1) & \cdots & u_N(1) \\ \vdots & \ddots & \vdots \\ u_1(N) & \cdots & u_N(N) \end{pmatrix}$ ,

$u_l = (u_l(1), \dots, u_l(N))^T$  represents the  $l$ -th eigenvector,  $u(l) = \{u_1(l), \dots, u_N(l)\}$  represents row vector consisting of the values of all eigenvectors at position  $l$ . For convenience, "node with the indices  $n$ " is denoted by "node  $n$ ".  $j$  is the imaginary unit.

#### 4.1.1 Overall Claim

Before making a mathematical proof, we first claim that:

**Claim 1.** Among all inputs required by GCN, the position of node  $\alpha$  is determined by  $u(\alpha)$ .

#### 4.1.2 Node signal model

Firstly, we give the Fourier domain coordinates of the signal of a single node at a specific frequency:

**Proposition 1.** Given a frequency  $\nu$ , the coordinates in the Fourier domain of signal of node  $\alpha$  is:

$$\hat{f}_\alpha[\nu] = \sum_{t=0}^{E-1} \bar{\theta}_t \left( \sum_{i=1}^N c_i e^{\lambda_i t} u_i(\alpha) \right) e^{-j \frac{2\pi}{E} \nu t}, \quad (14)$$

where  $\bar{\theta}_t$  and  $c_i$  is constants,  $E$  is the total training epoch.

**Proof 1.** The signal variation of a single node with  $E$  epochs is presented as  $f[0], f[1], \dots, f[E-1]$ . According to the Discrete Fourier Transform (DFT) theory, given a frequency  $\nu$ , the Fourier transform for the signal  $f$  of node  $\alpha$  (before introducing trainable parameters) is

$$\hat{f}_\alpha[\nu] = \sum_{t=0}^{E-1} f_\alpha[t] e^{-\frac{2\pi}{E} \nu t j}, \quad (15)$$

further, in the Fourier domain, according to the aggregation theory on graph [23], the signal in Fourier domain is dynamically vibrates caused by trainable parameters, so here we introduce a constant matrix representing vibration frequency  $\theta \sim \mathbb{R}^E$  where  $\theta_i$  is the value of  $\theta$  at the  $i$ th node, by act  $\bar{\theta}$  on all frequency  $\hat{f}[\nu], \nu = 0 : E-1$  at every epochs, the signal fitted by  $\bar{\theta}$  will be obtained, as shown in the figure 4 specifically.

Hence the Fourier domain graph signal (after introducing trainable parameters) is

$$\hat{f}_\alpha[\nu] = \sum_{t=0}^{E-1} \bar{\theta}_i f_\alpha[t] e^{-\frac{2\pi}{E} \nu t j}. \quad (16)$$

Further, according to the model of signal transmission on the graph [34], the transmission of signal  $f$  on  $\mathcal{G}$  is proportional to  $\Delta$  acting on  $f$  with time  $t$ , as the end-to-end training drives the signal transmission on the graph, by regarding  $t$  as the end-to-end training epoch  $t$ , so

$$\frac{df}{dt} = -k\Delta f, \quad (17)$$

where  $k$  is a constant. Consider the first-order matrix ordinary differential equation [35], [36] is

$$\dot{\mathbf{x}}(t) = \mathbf{A}(t)\mathbf{x}(t), \quad (18)$$

where  $\dot{\mathbf{x}}$  is the vector of first derivatives of these functions, and  $\mathbf{A}(t)$  an  $N \times N$  matrix of coefficients. In the case where  $\mathbf{A}$  is constant and has  $N$  linearly independent eigenvectors, the general solution of Eq. (18) is

$$\mathbf{x}(t) = c_1 e^{\lambda_1 t} \mathbf{u}_1 + c_2 e^{\lambda_2 t} \mathbf{u}_2 + \dots + c_N e^{\lambda_N t} \mathbf{u}_N, \quad (19)$$

where  $\lambda_1, \dots, \lambda_N$  are the eigenvalues of  $\mathbf{A}$ ,  $\mathbf{u}_1, \dots, \mathbf{u}_N$ , as  $\Delta \sim \mathbb{R}^{N \times N}$  has  $N$  linearly independent eigenvectors similarly, so Eq. (17) is homogeneous to Eq. (18), which general solution is

$$f_\alpha[t] = \sum_{i=1}^N c_i e^{\lambda_i t} u_i(\alpha), \quad (20)$$

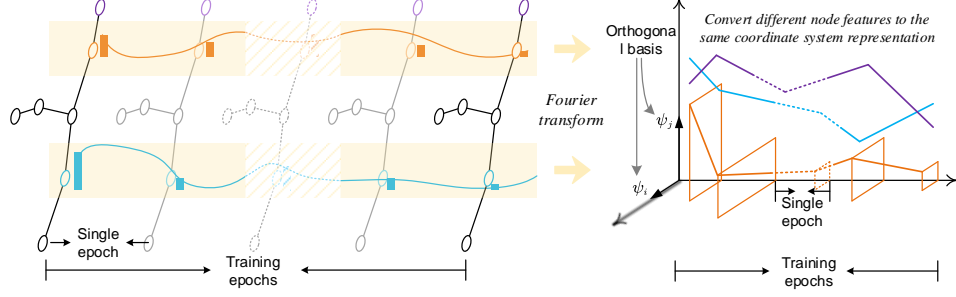


Fig. 3. The method of building node signal model. We regard the node feature change with the training epoch as the independent signal vibration, and transform all the signals to a unified orthogonal basis by Fourier transform.

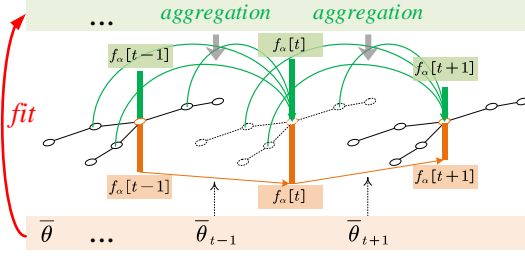


Fig. 4. Using  $\bar{\theta}$  to fit graph quantify aggregation.

which can be regard as the global change model of graph signal transmission, hence Eq. (14) can be acquired by substituting Eq. (20) into Eq. (16).

Then, for node  $\alpha$ , we integrate the signals of all frequencies in the Fourier domain to obtain the original signal in the orthogonal basis representation which is stated in the following proposition.

**Proposition 2.** The signal of node  $\alpha$  in epoch  $t$  is:

$$f_\alpha[t] = \sum_{\nu=0}^{E-1} \frac{2}{E} \left| \hat{f}_\alpha[\nu] \right| \cos \left[ (2\pi\nu/E\epsilon) t\epsilon + \arg(\hat{f}_\alpha[\nu]) \right] e^{j\frac{2\pi}{E}\nu t}, \quad (21)$$

where  $\arg$  is the argument of a complex number,  $\epsilon$  denotes the epoch interval, here we take is as a minimal value, that is,  $\epsilon \rightarrow 0$ .

**Proof 2.** According the Discrete Fourier Transform (DFT) theory, The inverse transform of  $\hat{f}_\alpha[\nu]$  is

$$f_\alpha[t] = \frac{1}{E} \sum_{\nu=0}^{E-1} \hat{f}_\alpha[\nu] e^{j\frac{2\pi}{E}\nu t} \quad (22)$$

i.e. the inverse matrix is  $\frac{1}{N}$  times the complex conjugate of the original (symmetric) matrix.

Note that the  $\hat{f}_\alpha[\nu]$  coefficients are complex. We can assume that the graph signal  $f[t]$  values are real (this is the simplest case; there are situations (e.g. radar) in which two inputs, at each  $t$ , are treated, as a complex pair, since they are outputs from  $0^\circ$  and  $90^\circ$  demodulators).

In the process of taking the inverse transform the term  $\hat{f}_\alpha[\nu]$  and  $\hat{f}_\alpha[E-\nu]$  (the spectrum is symmetrical about  $\frac{E}{2}$  [37]), combine to produce 2 frequency components,

only one of which is considered to be valid. Hence from the Eq. (22), the contribution to  $f_\alpha[t]$  of  $\hat{f}_\alpha[\nu]$  and  $\hat{f}_\alpha[E-\nu]$  is:

$$C_\alpha^\nu[t] = \frac{1}{E} \left( \hat{f}_\alpha[\nu] e^{j\frac{2\pi}{E}\nu t} + \hat{f}_\alpha[E-\nu] e^{j\frac{2\pi}{E}(E-\nu)t} \right), \quad (23)$$

as all graph signal  $f[t]$  is real,

$$\hat{f}_\alpha[E-\nu] = \sum_{t=0}^{E-1} f[t] e^{-j\frac{2\pi}{E}(E-\nu)t}, \quad (24)$$

as according to the Euler's formula [38],

$$e^{-j2\pi t} = \frac{1}{\cos(2\pi t) + j \sin(2\pi t)} = 1, \text{ s.t. } t \in \mathbf{N}_+. \quad (25)$$

we have

$$e^{-j\frac{2\pi}{E}(E-\nu)t} = \underbrace{e^{-j2\pi t}}_{1 \text{ for all } t} e^{+j\frac{2\pi}{E}\nu t} = e^{+j\frac{2\pi}{E}\nu t}, \quad \text{i.e. } \hat{f}_\alpha[E-\nu] = \hat{f}_\alpha^*[\nu], \quad (26)$$

where  $\hat{f}_\alpha^*[\nu]$  is the complex conjugate, substituting Eq. (26) into Eq. (23), as  $e^{j2\pi t} = 1$  (refer to Eq. (25)) we have

$$\begin{aligned} C_\alpha^\nu[t] &= \frac{1}{E} \left( \hat{f}_\alpha[\nu] e^{j\frac{2\pi}{E}\nu t} + \hat{f}_\alpha^*[\nu] e^{-j\frac{2\pi}{E}\nu t} \right) \\ &= \frac{2}{E} \left[ \text{Re}(\hat{f}_\alpha[\nu]) \cos(2\pi\nu t/E) - \text{Im}(\hat{f}_\alpha[\nu]) \sin(2\pi\nu t/E) \right] \\ &= \frac{2}{E} |F[\nu]| \cos \left[ (2\pi\nu/E\epsilon) t\epsilon + \arg(F[\nu]) \right], \end{aligned} \quad (27)$$

hence, by integrate the signals of all frequencies  $\nu = 0 : E-1$

$$f_\alpha[t] = \sum_{\nu=0}^{E-1} C_\alpha^\nu[t] e^{j\frac{2\pi}{E}\nu t} \quad (28)$$

Eq. (21) can be obtained by substituting Eq. (27) into Eq. (28).

#### 4.1.3 Start-up GCN

We build the GCN process on the mathematical model given by section 4.1.2. In this section, we first obtain the initial state of the graph signal by blocking the signal transmission which is stated in the following proposition.

**Proposition 3.** The initial signal of node  $\alpha$  is

$$f_\alpha[0] = 2\bar{\theta}_0 \text{Sum}[u(\alpha)], \quad (29)$$

where Sum denotes the sum of all elements.

**Proof 3.** According to the General GCN forward propagation [39], the embedding feature of  $\mathcal{G}$  is

$$f^e[\cdot] = \sigma \left( U g_\theta(\Lambda) U^\top f \right), \quad (30)$$

where  $g_\theta(\Lambda) = \text{Diag}(\theta_1, \dots, \theta_N)$  is the trainable diagonal matrix, hence, the output of GCN for node  $\alpha$  is

$$f_\alpha^e[\cdot] = u(\alpha) g_\theta(\Lambda) U^\top f, \quad (31)$$

considering that there is no direct relationship between the node features distribution and the graph structure, so, by denoting  $g_\theta(\Lambda) U^\top$  as a constant matrix  $\Phi \in \mathbb{R}^{N \times d}$  where  $d$  is the dimension of the feature,  $\phi_i$  is the  $i^{\text{th}}$  row of  $\Phi$ ,  $\phi_i(k)$  is the  $k^{\text{th}}$  element of  $\phi_i$ . In  $d = 1$  case,

$$f_\alpha^e[\cdot] = \sum_{i=1}^N \phi_1(i) u_i(\alpha), \quad (32)$$

in  $d > 1$  case,

$$f_\alpha^e[\cdot] = \left[ \sum_{i=1}^N \phi_1(i) u_i(\alpha), \dots, \sum_{i=1}^N \phi_d(i) u_i(\alpha) \right]. \quad (33)$$

Since our aim is to solve the qualitative problem of node localization, we only give the case of  $d = 1$ , as the discovery making from observation: Eq. (32) is homogeneous with Eq. (20), moreover  $\phi_i$  and  $c_i$  both denote the changeable parameter, we conclude that proposition 2 and proposition 3 is applied to the training process of GCN.

we consider the initial state as the non-transmission state, that is, for node  $\alpha$ ,  $f_\alpha[0] = \dots = f_\alpha[E - 1]$ , hence, the transmission of graph signal can be blocked by letting  $c_i = e^{-\lambda_i t}$ , by regard the initial status of GCN as  $E = 1$ ,  $t = 0$ , Eq. (29) can be obtained by substituting Eq. (14) into Eq. (21), *s.t.*  $E = 1$ ,  $t = 0$ .

Next, we start up the message passing on  $\mathcal{G}$ . As  $\bar{\theta}$  denotes constants, Eq. (14) can be concluded by

$$\hat{f}_\alpha[\nu] = \sum_{t=0}^{E-1} \left( \sum_{i=1}^N \bar{c}_i e^{\lambda_i t} u_i(\alpha) \right) e^{-j \frac{2\pi}{E} t \nu}, \quad (34)$$

where  $\bar{c}_i = \bar{\theta}_t c_i$ , by substituting Eq. (34) into Eq. (21), the final expression of node signal is:

$$f_\alpha[t] = \lim_{\epsilon \rightarrow 0} \sum_{\nu=0}^{E-1} \frac{2}{E} \left| \sum_{t=0}^{E-1} \left( \sum_{i=1}^N \bar{c}_i e^{\lambda_i t} \underbrace{u_i(\alpha)}_{\text{from } \mathcal{E}} \right) e^{-j \frac{2\pi}{E} t \nu} \right| \cos \left[ (2\pi \nu / E \epsilon) t \epsilon + \arg(\hat{f}_\alpha[\nu]) \right] e^{j \frac{2\pi}{E} t \nu}, \quad (35)$$

Equation 35 gives the signal model of all nodes in the unified reference frame, by observing equation 35, for node  $\alpha$ , among all the initial conditions related to  $\mathcal{G}$ , only  $u(\alpha)$  appears in the process of node signal change. In other words, in the elastic system brought by end-to-end training, only  $u(\alpha)$  is a controllable factor, so we simplify the above equation to

$$f_\alpha[t] = \mathcal{F}[u(\alpha)], \quad (36)$$

and the feature vibrate of node  $\alpha$  under the end-to-end training is

$$\begin{aligned} \text{Initial: } & 2\bar{\theta}_0 \text{Sum}[u(\alpha)] \\ \text{Training: } & \mathcal{F}[u(\alpha)] \end{aligned}$$

So we come to the claim 1 according to all the reasons above.

## 4.2 Basic model

According to the claim in section 4.1, we denote each row of the Laplacian matrix as an independent generating target. We use the spectral graph convolution (without any constraints and simplification rules) [3] as the basic model, and take it as an encoder. We use an extra fully connected neural network decoder. That is, denote the basic forward propagation as:

$$f^e = \sigma \left( U g_\theta(\Lambda) U^\top f \right) \quad (37a)$$

$$y_{out} = f^e W^D \quad (37b)$$

In Eq. (37),  $U$  contains the information of the edges in the graph, we will replace it with a matrix generated from Gaussian noise. Eq. (37) is the basic signal forward propagation. Next, we will describe how to improve Eq. (37), thus let the base model can accommodate the generated node position.

## 4.3 Generating the node position from noise

When  $u(n)$  is completely generated by noise, the specific points will keep anonymous. So we make  $u(n)$  as the generation target, and the output of the generator is  $u^G(n)$ , which tries to approximate the underlying true node position distribution.

Next, we define a probability density function (PDF) for input noise. In order to enable the generator to locate a specific point, the input noise of the generator will be constrained by the position of the target point. So we define the input noise as having a PDF equal to that of Staggered Gaussian distribution, the purpose is to make the noise not only satisfy the Gaussian distribution but also do not coincide with each other, thus densely distributed on the number axis.

**Proposition 4.** (Staggered Gaussian distribution). Given a minimum probability  $\epsilon$ ,  $N$  Gaussian distributions centered on  $x = 0$  satisfy  $P(x, n) \sim \text{Norm}(2\sigma(2n - N - 1)\sqrt{\log(\sqrt{2\pi}\sigma\epsilon)}, \sigma^2)$ , so that the probability density function of each distribution is greater than  $\epsilon$ . Where Norm represents the Gaussian distribution,  $n$  represents the node number,  $\sigma$  represents the standard deviation, and  $\epsilon$  represents the set minimum probability.

**Proof 4.** Given a probability density function  $h(x_p)$  of the Gaussian distribution  $\text{Norm}(\mu_p, \sigma^2)$ , when  $h(x_p) = \epsilon$ ,

$$x_p = \mu_p \pm 2\sigma \sqrt{\log \left( \sqrt{(2\pi)\sigma\epsilon} \right)} \quad (38)$$

Let  $2\sigma \sqrt{\log(\sqrt{(2\pi)\sigma\epsilon})} = r$  as the distance from the average value  $\mu_p$  to maximum and minimum value of  $x_p$ . Specify that each  $x_p$  represents the noise distribution of each node. In order to make all the distribution staggered

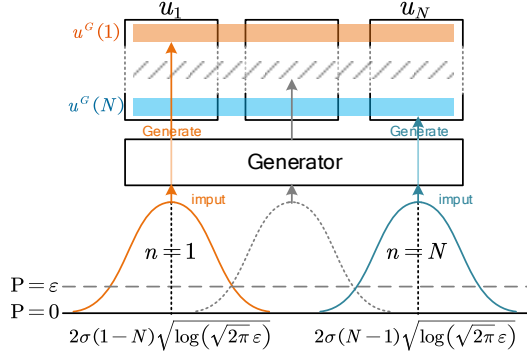


Fig. 5. Generator with Staggered Gaussian distribution as input

and densely arranged, stipulate  $\max(x_p) = \min(x_{p+1})$ , and keep all distributions symmetrical about  $x = 0$ . So, when the total number of nodes is  $N$ ,  $\mu_1 = (1 - N)r$ ,  $\mu_2 = (3 - N)r, \dots, \mu_N = (N - 1)r$ , that is,  $\mu_n = (2n - N - 1)r = 2\sigma(2n - N - 1)\sqrt{\log(\sqrt{2\pi}\epsilon)}$ .

The process of generating sample  $u^G(v)$  from Staggered Gaussian noise  $Z_v \sim P(x, v)$  is expressed as  $u^G(v) = G(Z_v; \theta^G)$ , where  $\theta^G$  denotes the weight of  $G$ , and  $U$  generated by  $G$  denoted as  $U^G$ . The process of generator is as shown in Fig. 5.

#### 4.4 Detecting the generated position

##### Algorithm 1 AN-GCN

**Require:** Weights of  $D$ :  $\theta^D$ , include  $g_\theta^{D,enc}(\Lambda)$  is used for encoding,  $\theta^{D,dec}$  is used for decoding. Weights of  $G$ :  $\theta^G$ .

Training epoch of  $D$  and  $G$ .

- 1: Initialize  $U^D = U$
- 2: **for** epoch in Train epochs for  $D$  **do**
- 3: Random sample a node  $v$
- 4: Obtain noise  $Z_v$  from  $P(z, v)$
- 5:  $u^G(v) \leftarrow G(Z_v^D)$  // Generate
- 6:  $U_{\cdot v}^D = U_{\cdot v}^D + q(u^G(v) - U_{\cdot v}^D)$  // Linear approximation
- 7: Calculate fake label of  $v$  by Eq. (42a)
- 8: Calculate real label of  $v$  by Eq. (42b)
- 9: Calculate  $\nabla_{update}^D$  by Eq. (43)
- 10:  $\theta^D \leftarrow \theta^D - \nabla_{update}^D$
- 11: **for** epoch in Train epochs for  $G$  **do**
- 12: Obtain noise  $Z_v$  from  $P(z, v)$
- 13: Calculate  $y_v^{fool}$  by Eq. (44)
- 14: Calculate  $\nabla_{update}^G$  by Eq. (46)
- 15:  $\theta^G \leftarrow \theta^G - \nabla_{update}^G$
- 16: **end for**
- 17: **end for**

**Ensure:** Trained generator weights  $\theta^G$ .

After proposing the generation of  $u^G(n)$ , we need to set discriminator  $D$  to evaluate the quality of  $u^G(n)$  generated by generator  $G$ , and design the two-player game in order to make  $u^G(n)$  can complete the accurate node classification.

To ensure the accuracy of classification, we use classification quality as an evaluation indicator to drive the entire GAN, so in the game process,  $D$  can not only distinguish

the adversarial samples generated by  $G$  (non-malicious, used for anonymize node), but also ensure the accuracy of node classification through the adversarial training with the classification accuracy as the final optimization objective. Specifically,  $D$  is divided into two parts: a diagonal matrix with trainable parameters  $D_{enc}$  used for encode (embed) the graph, and a parameter matrix  $D_{dec}$  used for decode, their are  $g_\theta^{D,dec}(\Lambda)$  and  $\theta^{D,enc}$ , respectively. Thus the forward propagation become

$$f^e = \sigma \left( U D_{enc} U^\top f \right) D_{dec} \quad (39)$$

Consider there are two  $U$  in the encoder (Eq. (37a)), we mark them as:

$$f^e = \sigma \left( U^G D_{enc} U^D f \right) D_{dec}, \quad (40)$$

that is, the corresponding  $u(\cdot)$  to  $U^G$  is generated by independent generation of different rows, and the  $U^D$  on the right is approximate linearly according to the numerical change of left  $U$ . Consider that  $U^G$  and  $U^D$  changed dynamically while training, we use  $U^{G,e}$  and  $U^{D,e}$  denote  $U^G$  and  $U^D$  in epoch  $e$ . While generate row  $l$  of  $U^G$ , the corresponding column of  $U^D$  (denote as  $u_l^D$ ) linear approximate towards  $u^G(l)$ . Specifically, the general term formula for its value in training epoch  $e$  is

$$u_l^{D,e} = \begin{cases} u_l, & s.t. e = 1 \\ u_l^{D,e-1} + q \left( u^{G,e}(l) - u_l^{D,e-1} \right), & s.t. e > 1 \end{cases},$$

where  $u^{G,e}(l)$  is the generated  $u^{G,e}(l)$  in epoch  $e$ ,  $q$  is the custom linear approximation coefficient. Thus,  $U^{D,e}$  is gradually approaches the generator matrix  $U^{G,e}$  during the training process. The relationship between two  $U$  at different positions and  $G$  is shown in the Fig. 4.4.

After all, the basic model is improved as Fig 4.4:

Next, let  $f^{e,G}(v)$  and  $f^{e,D}(v)$  denote the embedding of the node  $v$  when using  $u^G(v)$  and  $u(v)$  locate nodes at epoch  $e$ , respectively. It can be seen that the purpose of adversarial training is to make  $f^{e,G}(v)$  and  $f^{e,D}(v)$  as similar as possible. In each training epoch  $e$ , first we obtain  $u^G(v)$  and  $U^{D,e}$  related to the target node  $v$ . Specifically, generate the  $u^G(v)$  from the Staggered Gaussian noise corresponding to node  $v$ , and update the corresponding column of  $U^{D,e-1}$  to  $U^{D,e}$ . Second, we use  $D_{enc}$  and  $D_{dec}$  to evaluate the quality of this epoch of generators, by get the node embedding  $f^{e,G}(v)$  of  $v$  through  $D_{enc}$ , decode  $f^{e,G}(v)$  through  $D_{dec}$  to get the label possibility  $y_v^{fake}$ . Consider we need to calculate specific node embedding, based on Eq. (37a), the embedding of node  $v$  is

$$f^e(v) = \sigma \left( u(v) g_\theta(\Lambda) U^\top f \right) \quad (41)$$

thus the calculation of  $y_v^{fake}$  and  $y_v^{real}$  is:

$$y_v^{fake} = u^G(v) D_{enc} U^D f(v) D_{dec} \quad (42a)$$

$$y_v^{real} = u(v) D_{enc} U f(v) D_{dec}. \quad (42b)$$

Third, calculate the loss functions of  $y_v^{real}$  and  $y_v^{fake}$  respectively, and update the weight of  $D$  according to the gradient. The loss function of  $D$  is designed as:

$$\text{Loss}_D(y) = \begin{cases} \mathbb{C}[\mathbb{S}(y), \text{label}_v], & s.t. y = y_v^{real} \\ \mathbb{C}[\mathbb{S}(y), \text{SP}(\{\text{label}_\gamma | \gamma \neq v\})], & s.t. y = y_v^{fake} \end{cases},$$

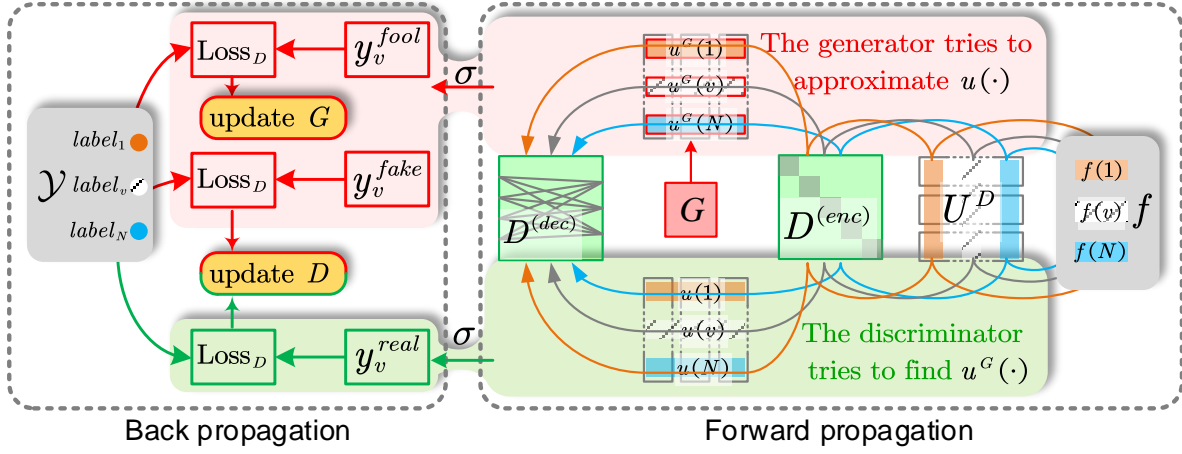


Fig. 6. The schematic illustration of AN-GCN

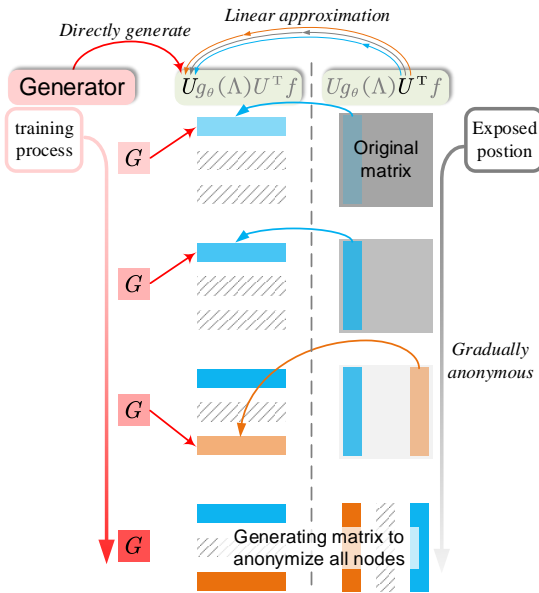


Fig. 7.

$$y_{out} = \sigma(U_{g_{\theta}(\Lambda)} U^T f) W^D$$

Discriminator  
Approximate To  $U^T$  linearly  
Generated by  $G$

Fig. 8.

where  $label_i$  represents the true label of node  $i$  (one-hot),  $\mathbb{C}$  denotes Cross entropy function,  $\mathbb{S}$  denotes Sigmoid function, SP denotes Random sampling. Next, update the gradient of  $D$  according to  $\text{Loss}_D(y)$ :

$$\nabla_{update}^D = \nabla_{g_{\theta}^{D,dec}(\Lambda), \theta^{D,enc}} [\text{Loss}_D(y_v^{real}) + \text{Loss}_D(y_v^{fake})]. \quad (43)$$

Next, aiming that letting  $u^G(v)$  generated by  $G$  can provide accurate classification, we train  $G$ . After re-sample noise for  $Z_v$ , the label used to fool  $D$  is calculated by

$$y_v^{fool} = G(Z_v) D_{enc} U^D f D_{dec}, \quad (44)$$

in generation epoches, the loss function of  $D$  is designed as:

$$\text{Loss}_D(y) = \mathbb{C}[\mathbb{S}(y), label_v], s.t. y = y_v^{fool} \quad (45)$$

further update the weight of  $G$  according to the output of  $D$

$$\nabla_{update}^G = \nabla_{\theta^G} [\text{Loss}_D(y_v^{fool})] \quad (46)$$

in order to make the output of  $G$  is classified as the real sample by  $D$ .

The schematic illustration of AN-GCN is represented by fig 6, and the algorithm process of AN-GCN is given in the algorithm 1,

## 5 EVALUATION

We report results of experiments with two widely used benchmark data sets for node classification, which include CORA [40], [41], CITESEER [42], either used with extensive research of graph adversarial attack and defense [30], [43], [44].

### 5.1 Evaluation For Proposed Attack Method

By observing the effectiveness of the attack model, we further prove that the exposure of node position is the main reason for graph vulnerability (Eq.9).

The evaluation for the attack effect of Eq. 8 includes five items: 1. The effectiveness of the attack (represented by box plot, Let Eq. 8 act on the Semi-GCN [25] which trained on the clean graph to get  $\mathcal{G}_{victim}$ , evaluate the classification of  $\mathcal{G}_{victim}$ ). 2. Transferability of attack (transfer  $\mathcal{G}_{victim}$  to the training set of GraphSAGE, GAT, GCN ChebNet [3], thus get the  $\mathcal{G}_{victim}$  and evaluate the classification performance of  $\mathcal{G}_{victim}$  by various model). 3. Attack effect on the existing mainstream defense scheme (Deep Robust [45]). The process is the same as that of evaluation 1, and the target model becomes Deep Robust), 4. Concealment of a single node attack. The evaluation index is expressed as to whether there is an obvious perturbation in the 5th order neighborhood of the target node. 5. The stability of graph structure after the attack (represented by degree distribution [5]). The results are shown in Fig. 9. In particular, the results of the evaluation item 1, 2 and 3 above are presented in Table 1

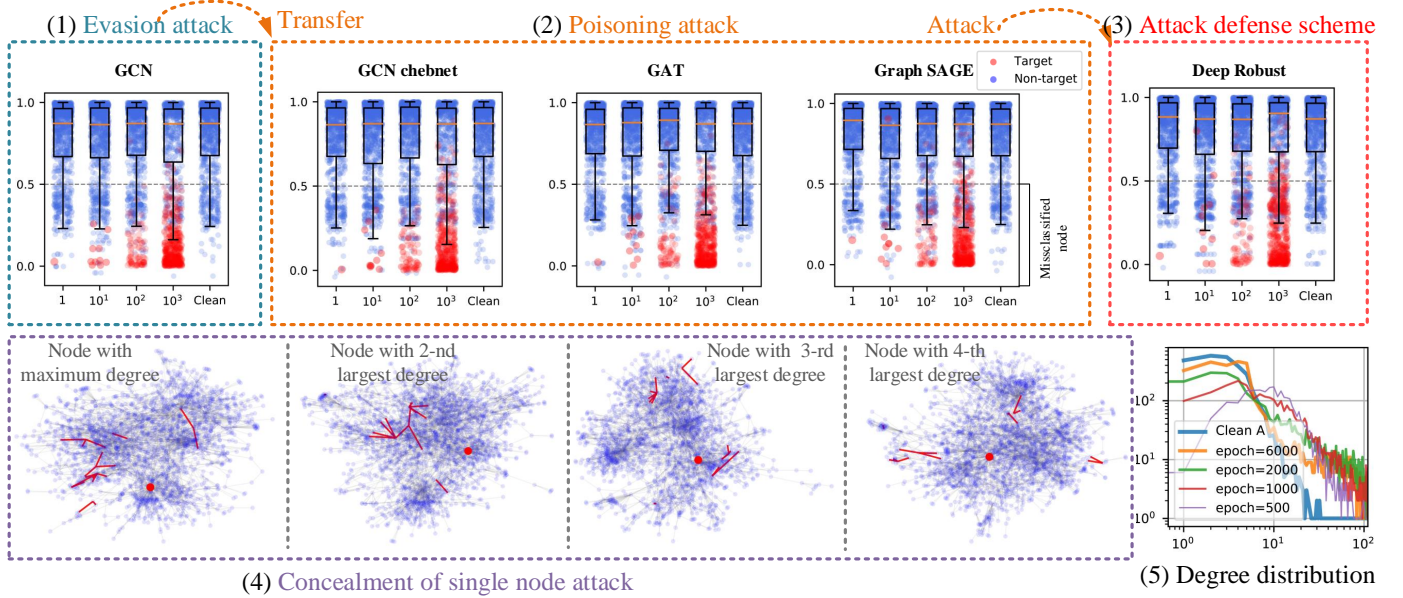


Fig. 9. The evaluation result of the attack method represented by Eq. 8. (1). Evaluation 1. The horizontal axis is the number of attack nodes, and the vertical axis is the scaling index according to the loss function. The more similar the distribution of non-target nodes and clean graph, the less misclassified non-target nodes will be. It can be seen that with the increase of the number of attacks, almost all the target nodes are misclassified, while the non-target nodes almost keep the original classification results. (2). Evaluation 2. After  $\mathcal{G}_{victim}$  was transferred to different models and retrained, the performance of each model was evaluated. It can be seen that all models are successfully attacked, which shows that the attack method represented by Eq. 8 can transfer to other models. (3). Evaluation 3. it can be seen that a large number of target nodes are misclassified, thus prove the defense ability of the model decreases. (4). Evaluation 4. The red dot is the target node, and the red line is the modified connection. As can be seen that we have not directly modified the node, and the total number of perturbations is insignificant, so the attack has well performance on concealment. (5). Evaluation 5. With the increase of training epoch, the degree distribution is more and more like the degree distribution of clean A, that is to say,  $\mathcal{G}_{victim}$  will eventually tend to be stable.

TABLE 1

the results of the evaluation item 1, 2 and 3, Success rate represents the probability that the target node is successfully misclassified

success rate %	Target number			
	1	10	100	1000
GCN	100	100	96	93.1
GCN_ChebNet	100	100	100	96.3
GAT	100	100	95	91.5
GraphSAGE	100	80	96	89.4
DeepRobust	100	60	74	72.8

## 5.2 Evaluation for the claim

We designed two experiments to verify the Claim 1. In Experiment 1, we observe the position deviation of nodes in the embedded space after the disturbance is applied to the corresponding  $u(\cdot)$ , if the deviation of node  $v$  is significantly larger than that of other points while applied to  $u(v)$ , it shows that  $u(v)$  is highly sensitive to the position of  $v$ , thus proves the effectiveness of Claim 1. In Experiment 2, we observe the change for the  $u(\cdot)$  of neighbors after deleting a node. If with the increase of neighbor order (distance from the deleted node), the change of corresponding  $u(\cdot)$  show less significance, then it further shows that the specific location of  $v$  is closely related to the value of  $u(v)$ . Both experiment 1 and 2 prove the theoretical correctness of Claim 1 collectively.

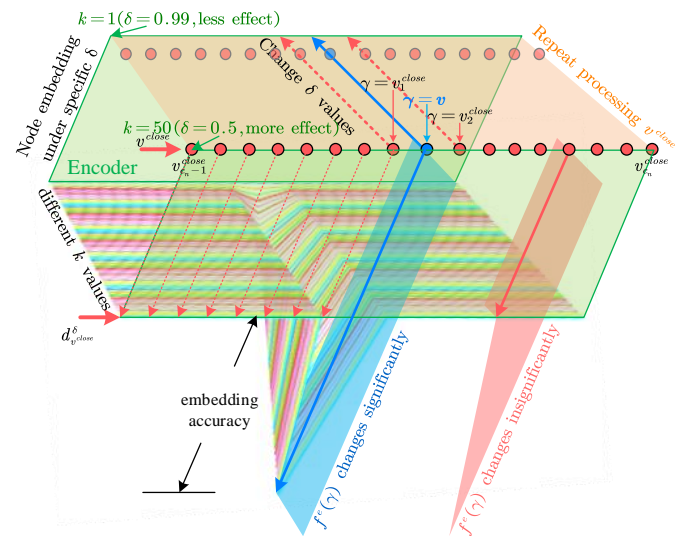


Fig. 10. the deviation of node embedding after disturb the  $u(\cdot)$  corresponding to neighbors. Only when  $\delta$  acts on the target point  $v$ , the embedding accuracy will suddenly drop (measured by the Euclidean distance between  $f^e(v)$  and  $f^{e,\delta}(v)$ ), and the other conditions will remain stable.

### 5.2.1 Experiment 1

By selecting a target node  $v$ , the deviation of  $v$  in the embedding space is observed by applying a small disturbance to the  $u(\cdot)$  for neighbors of  $v$ . Let  $\text{Nbor}_{1^{\text{th}}}(v) = \{v_1(1), \dots, v_1(c_v)\}$  denotes the 1<sup>st</sup>-order neighbors of  $v$ , given a factor  $\delta$ , the embedding deviation of  $v$  is calculated

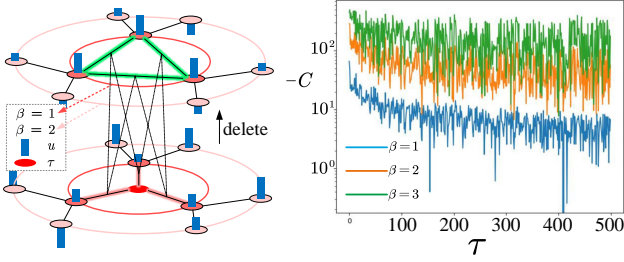


Fig. 11. Deviation of  $u(\cdot)$  in different positions after deleting nodes. After deleting  $\tau$ , the change of neighbor  $u^{(d)}(\tau_\beta(\cdot))$  of different orders  $\beta$  of  $\tau$  (right). After deleting node  $\tau$ , the overall difference in the change of  $u^{(d)}(\tau_\beta(\cdot))$  for each order neighbor is large, and the  $u(\cdot)$  of the first-order neighbor  $u^{(d)}(\tau_\beta(\cdot))$  has the largest change (the vertical axis is  $-C$ ). In other words, after the node  $\tau$  is deleted, the  $u(\cdot)$  corresponding to its first-order neighbor the  $u(\tau_1(\cdot))$  has changed significantly, while the  $u(\tau_2(\cdot))$  and  $u(\tau_3(\cdot))$  has changed less and showed a decreasing trend. Since deleting node  $\tau$  significantly affects the position of its first-order neighbors, as the order increases, the degree of influence gradually decreases, so the change of its  $u(\tau_\beta(\cdot))$  also gradually decreases.

by acting  $\delta$  on  $\text{Nbor}_{1^{\text{th}}}(v)$  successively, thus in every acting turn, given a target  $v_i^{\text{close}}$  original  $U$  become a disturbed matrix  $\hat{U}^{\delta, c_v}$ , which all rows in  $\hat{U}^{\delta, c_v}$  satisfy

$$\hat{u}^{\delta, c_v}(i) = \begin{cases} u(i), & \text{s.t. } i = v_1(i) \\ \delta u(i), & \text{s.t. } i \neq v_1(i) \end{cases}, \quad (47)$$

then embed  $f$  to embedding space by  $\hat{U}^{\delta, c_v}$  and a well-trained  $g_\theta(\Lambda)$ , by using Eq. (37a), embedding features under disturb is

$$f^{e, \delta} = \hat{U}^{\delta, c_v} g_\theta(\Lambda) (\hat{U}^{\delta, c_v})^\top f. \quad (48)$$

Further, we calculate the Euclidean distance [46] between  $f^{e, \delta}$  and  $f^e$  (Eq. (37a))

$$d_v^\delta = \|f^{e, \delta} - f^e\|_2 \quad (49)$$

while changing  $\delta$ , Using Chebyshev polynomial [3] as the convolution kernel, and Cora as the test data set, set  $c_v = 14$ ,  $\delta = 1 - \frac{k}{100}$ ,  $k \in \{1, \dots, 50\}$ . the result is shown as Fig.10, it can be seen  $u(v)$  has a greater impact on the embedding of node  $v$ .

### 5.2.2 Experiment 2

Delete a node  $\tau$  in the graph  $\mathcal{G}$  to obtain the deleted graph  $\mathcal{G}_\tau^{(d)}$ , and calculate the laplacian matrix  $L_\tau^{(d)} \sim \mathbb{R}^{(N-1) \times (N-1)}$  and matrix eigenvalues  $U_\tau^{(d)} = \{u^{(d)}(1), \dots, u^{(d)}(N-1)\} \sim \mathbb{R}^{(N-1) \times (N-1)}$ . To keep  $\mathcal{G}_\tau^{(d)}$  will be connected, All edges connected to  $\tau$  will be re-connected by traversal. Specifically, we stipulate that  $\omega_{ij}$  is the weight of connecting nodes  $i$  and  $j$  in  $\mathcal{G}$ , and  $\omega_{ij}^{(d)}$  corresponds to graph  $\mathcal{G}_\tau^{(d)}$ . The calculation method of all edge weights in  $\mathcal{G}_\tau^{(d)}$  is:

$$\omega_{ij}^{(d)} = \begin{cases} \omega_{ij}, \omega_{\tau i} = 0 \text{ or } \omega_{\tau j} = 0 \\ \omega_{ij} + \frac{\omega_{\tau i} + \omega_{\tau j}}{2}, \omega_{\tau i} \neq 0, \omega_{\tau j} \neq 0 \end{cases}. \quad (50)$$

After obtaining the fully connected  $\mathcal{G}_\tau^{(d)}$ , we recalculate corresponding  $U_\tau^{(d)}$ , and query all  $\beta^{\text{th}}$ -order neighbors of  $\tau$ :  $\text{Nbor}_{\beta^{\text{th}}}(\tau) = \{\tau_\beta(1), \tau_\beta(2), \dots\}$ , and obtain a list  $u(\tau_\beta(1)), \dots, u(\tau_\beta(N-1))$  after delete edges, which denote

as  $u^{(d)}(\tau_\beta(\cdot))$ . The quantitative representation of the change between the two is as follows

$$C \left[ u(\tau_\beta(\cdot)), u^{(d)}(\tau_\beta(\cdot)) \right] = \sum_{i=1}^{N-1} \left[ \log |u_i(\tau_\beta(\cdot))|^2 - \log |u_i^{(d)}(\tau_\beta(\cdot))|^2 \right]. \quad (51)$$

Replace different  $\beta$  and calculate  $C$ , the result is as shown in Figure 11. We select the first 500 nodes according to the number of connections from large to small. Figure 11 prove that the position of node  $\tau$  is inseparable from  $u(\tau)$ .

### 5.3 Evaluation for AN-GCN

Next, we evaluated AN-GCN. We mainly evaluate the accuracy of AN-GCN. Its robustness to the perturbation of training set is as the secondary evaluation item, because the application scenario of AN-GCN is that the user can ensure that AN-GCN is trained on the clean graph, the poisoning attack scenario which training AN-GCN on the poisoned graph is not the main problem of this paper, but we still evaluated can GAN in AN-GCN weaken the perturbation of the training set.

First, we evaluate the accuracy of AN-GCN on Cora dataset. We hope that AN-GCN can output accurate node embedding while keeping the node position completely generated by the well-trained generator, so we use the accuracy of node embedding to evaluate the effectiveness of AN-GCN. Since the generator does not directly generate the node embedding but completes the node prediction task by cooperating with the trained discriminator, we denote the accuracy of the generator  $acc_G$  to be the accuracy of the node label through the position generated by  $G$ , and denote  $acc_D$  as the accuracy of the discriminator. Further, we use  $acc_{GCN}$  to denote the accuracy of single-layer GCN (the convolution kernel adopts symmetric normalized Laplacian matrix [25]) with the same kernel of  $D$  as a comparison. The results are shown in Fig. 12.

Second, we evaluate the robustness of AN-GCN to the attack on Cora and Citeseer dataset, by taking a comparative experimental model as Semi-GCN, GAT, and RGCN [12] (a model of defense attacks). The results are presented in Table 2. The meta-learning attack is the state-of-the-art accuracy under attack. When the perturbation increases, the accuracy gap between our method and other methods widens, clearly demonstrating the advantage of our method.

In our previous work [48], we have proved that in multi-class classification, using samples with other categories as the supervised samples of the generated samples will accelerate the convergence of GAN, similarly, the supervised samples of discriminator in AN-GCN are the same. Therefore, using GAN will not cause an excessive burden. Since the recent work (including attacks and defenses) has seldom discussed the time burden, in this paper, we will not discuss the time burden.

## 6 CONCLUSIONS

We proved that edge-read permission to GCN makes it vulnerable according to the proposed general attack model.

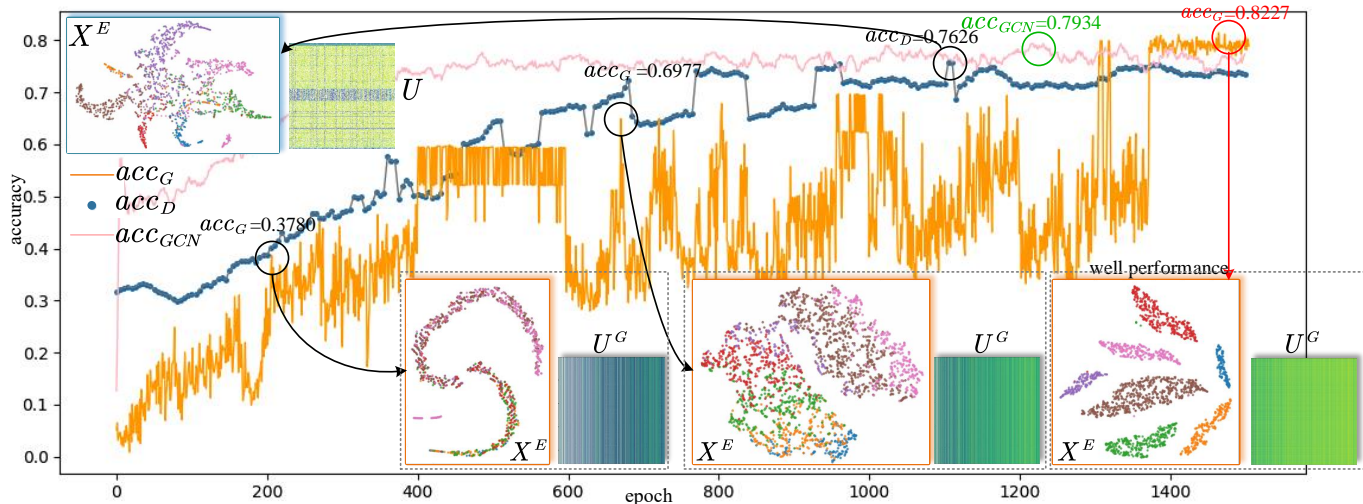


Fig. 12. Accuracy and visualization of node embedding during training, and visualization of node embedding. It can be seen that  $acc_D$  and  $acc_G$  are rising at the same time. When epoch  $> 1400$ ,  $acc_G$  remains at a high and stable state. We select  $G$  at epoch = 1475 as the final model selection, and the node embedding accuracy is 0.8227. In the 1500 epochs of training, the highest value of  $acc_{GCN}$  is 0.7934. The experimental results show that under the same convolution kernel design, AN-GCN not only effectively maintains the anonymity of the node, but also has a higher detection accuracy than only GCN 0.0293 higher.

TABLE 2  
Classification accuracy for various models after meta-learning attack [47]. P rate is the perturbation rate.

Dataset	P rate%	GCN	GAT	RGCN	AN-GCN
cora	0	83.43±0.40	<b>84.08±0.55</b>	83.19±0.64	81.03±0.59
	5	76.60±0.62	80.15±0.44	76.90±0.49	<b>80.92±0.43</b>
	10	70.52±1.33	75.03±0.35	72.35±0.42	<b>79.28±0.53</b>
	15	64.82±0.31	69.23±0.98	66.22±0.39	<b>79.10±0.60</b>
	20	59.02±2.52	59.03±1.03	59.01±0.29	<b>78.80±0.30</b>
	25	47.60±1.56	55.08±0.53	50.53±0.58	<b>77.90±0.70</b>
Citeseer	0	72.03±0.45	<b>73.63±0.62</b>	70.92±0.73	72.92±0.62
	5	71.88±0.32	<b>73.12±0.62</b>	71.51±0.63	72.53±0.43
	10	68.66±0.93	71.36±0.61	67.23±0.62	<b>72.28±0.61</b>
	15	65.51±0.59	69.98±0.32	66.09±0.82	<b>71.19±0.50</b>
	20	62.73±3.59	60.14±0.93	62.90±1.72	<b>70.01±0.61</b>
	25	56.73±2.50	60.90±1.36	56.43±0.72	<b>69.90±0.51</b>

Furthermore, we build the node signal model and give the node localization method of GCN. Finally, we withdraw the edge-read permission of GCN, so as to solve the vulnerability of GCN.

## REFERENCES

- [1] F. Monti, F. Frasca, D. Eynard, D. Mannion, and M. M. Bronstein, "Fake news detection on social media using geometric deep learning," *arXiv preprint arXiv:1902.06673*, 2019. 1
- [2] K. Shu, D. Mahudeswaran, S. Wang, and H. Liu, "Hierarchical propagation networks for fake news detection: Investigation and exploitation," in *Proceedings of the International AAAI Conference on Web and Social Media*, vol. 14, 2020, pp. 626–637. 1
- [3] M. Defferrard, X. Bresson, and P. Vandergheynst, "Convolutional neural networks on graphs with fast localized spectral filtering," in *Proceedings of the 30th International Conference on Neural Information Processing Systems*, 2016, pp. 3844–3852. 1, 7, 9, 11
- [4] H. Dai, H. Li, T. Tian, X. Huang, L. Wang, J. Zhu, and L. Song, "Adversarial attack on graph structured data," in *International conference on machine learning*. PMLR, 2018, pp. 1115–1124. 2
- [5] D. Zügner, A. Akbarnejad, and S. Günnemann, "Adversarial attacks on neural networks for graph data," in *Proceedings of the 24th ACM SIGKDD International Conference on Knowledge Discovery & Data Mining*, 2018, pp. 2847–2856. 2, 9
- [6] H. Chang, Y. Rong, T. Xu, W. Huang, H. Zhang, P. Cui, W. Zhu, and J. Huang, "A restricted black-box adversarial framework towards attacking graph embedding models," in *Proceedings of the AAAI Conference on Artificial Intelligence*, vol. 34, no. 04, 2020, pp. 3389–3396. 2
- [7] A. Bojchevski and S. Günnemann, "Adversarial attacks on node embeddings via graph poisoning," in *International Conference on Machine Learning*. PMLR, 2019, pp. 695–704. 2
- [8] B. Wang and N. Z. Gong, "Attacking graph-based classification via manipulating the graph structure," in *Proceedings of the 2019 ACM SIGSAC Conference on Computer and Communications Security*, 2019, pp. 2023–2040. 2
- [9] X. Tang, Y. Li, Y. Sun, H. Yao, P. Mitra, and S. Wang, "Transferring robustness for graph neural network against poisoning attacks," in *Proceedings of the 13th International Conference on Web Search and Data Mining*, 2020, pp. 600–608. 2
- [10] M. Jin, H. Chang, W. Zhu, and S. Sojoudi, "Power up! robust graph convolutional network against evasion attacks based on graph powering," *arXiv preprint arXiv:1905.10029*, 2019. 2
- [11] D. Zügner and S. Günnemann, "Certifiable robustness and robust training for graph convolutional networks," in *Proceedings of the 25th ACM SIGKDD International Conference on Knowledge Discovery & Data Mining*, 2019, pp. 246–256. 2
- [12] D. Zhu, Z. Zhang, P. Cui, and W. Zhu, "Robust graph convolutional networks against adversarial attacks," in *Proceedings of the 25th ACM SIGKDD International Conference on Knowledge Discovery & Data Mining*, 2019, pp. 1399–1407. 2, 11
- [13] Z. Deng, Y. Dong, and J. Zhu, "Batch virtual adversarial training for graph convolutional networks," *arXiv preprint arXiv:1902.09192*, 2019. 2
- [14] S. Wang, Z. Chen, J. Ni, X. Yu, Z. Li, H. Chen, and P. S. Yu, "Adversarial defense framework for graph neural network," *arXiv preprint arXiv:1905.03679*, 2019. 2
- [15] F. Feng, X. He, J. Tang, and T.-S. Chua, "Graph adversarial training: Dynamically regularizing based on graph structure," *IEEE Transactions on Knowledge and Data Engineering*, 2019. 2
- [16] Z. Wu, S. Pan, F. Chen, G. Long, C. Zhang, and S. Y. Philip, "A comprehensive survey on graph neural networks," *IEEE transactions on neural networks and learning systems*, 2020. 2
- [17] P. Cui, X. Wang, J. Pei, and W. Zhu, "A survey on network embedding," *IEEE Transactions on Knowledge and Data Engineering*, vol. 31, no. 5, pp. 833–852, 2018. 2
- [18] W. Huang, T. Zhang, Y. Rong, and J. Huang, "Adaptive sampling towards fast graph representation learning," *Advances in Neural Information Processing Systems*, vol. 31, pp. 4558–4567, 2018. 2
- [19] B. Perozzi, R. Al-Rfou, and S. Skiena, "Deepwalk: Online learning of social representations," in *Proceedings of the 20th ACM*

- SIGKDD international conference on Knowledge discovery and data mining, 2014, pp. 701–710. [2](#)
- [20] A. Grover and J. Leskovec, “node2vec: Scalable feature learning for networks,” in Proceedings of the 22nd ACM SIGKDD international conference on Knowledge discovery and data mining, 2016, pp. 855–864. [2](#)
- [21] J. Tang, M. Qu, M. Wang, M. Zhang, J. Yan, and Q. Mei, “Line: Large-scale information network embedding,” in Proceedings of the 24th international conference on World Wide Web, 2015, pp. 1067–1077. [2](#)
- [22] C. Yang, Z. Liu, D. Zhao, M. Sun, and E. Y. Chang, “Network representation learning with rich text information.” in Proceedings of the 24th International Joint Conference on Artificial Intelligence, vol. 2015, 2015, pp. 2111–2117. [2](#)
- [23] W. L. Hamilton, R. Ying, and J. Leskovec, “Inductive representation learning on large graphs,” in Proceedings of the 31st International Conference on Neural Information Processing Systems, 2017, pp. 1025–1035. [3, 5](#)
- [24] P. Veličković, G. Cucurull, A. Casanova, A. Romero, P. Lio, and Y. Bengio, “Graph attention networks,” in Proceedings of the 5th International Conference on Learning Representations, 2017. [3](#)
- [25] T. N. Kipf and M. Welling, “Semi-supervised classification with graph convolutional networks,” arXiv preprint arXiv:1609.02907, 2016. [3, 4, 9, 11](#)
- [26] K. Zhou, Y. Dong, W. S. Lee, B. Hooi, H. Xu, and J. Feng, “Effective training strategies for deep graph neural networks,” arXiv preprint arXiv:2006.07107, 2020. [3](#)
- [27] A. Loukas, “What graph neural networks cannot learn: depth vs width,” in International Conference on Learning Representations, 2019. [3](#)
- [28] L. Sun, Y. Dou, C. Yang, J. Wang, P. S. Yu, L. He, and B. Li, “Adversarial attack and defense on graph data: A survey,” arXiv preprint arXiv:1812.10528, 2018. [3](#)
- [29] J. Ma, S. Ding, and Q. Mei, “Towards more practical adversarial attacks on graph neural networks,” Advances in neural information processing systems, 2020. [3](#)
- [30] Y. Sun, S. Wang, X. Tang, T.-Y. Hsieh, and V. Honavar, “Non-target-specific node injection attacks on graph neural networks: A hierarchical reinforcement learning approach,” in Proceedings of the 29th international conference on world wide web, vol. 3, 2020. [3, 9](#)
- [31] A. Bojchevski and S. Günnemann, “Adversarial attacks on node embeddings via graph poisoning,” in International Conference on Machine Learning. PMLR, 2019, pp. 695–704. [3](#)
- [32] M. Fang, G. Yang, N. Z. Gong, and J. Liu, “Poisoning attacks to graph-based recommender systems,” in Proceedings of the 34th Annual Computer Security Applications Conference, 2018, pp. 381–392. [3](#)
- [33] X. Liu, S. Si, X. Zhu, Y. Li, and C.-J. Hsieh, “A unified framework for data poisoning attack to graph-based semi-supervised learning,” 2019. [3](#)
- [34] D. I. Shuman, S. K. Narang, P. Frossard, A. Ortega, and P. Vandergheynst, “The emerging field of signal processing on graphs: Extending high-dimensional data analysis to networks and other irregular domains,” IEEE signal processing magazine, vol. 30, no. 3, pp. 83–98, 2013. [5](#)
- [35] S. Khorasani and A. Adibi, “Analytical solution of linear ordinary differential equations by differential transfer matrix method.” Electronic Journal of Differential Equations (EJDE)[electronic only], vol. 2003, pp. Paper–No. 2003. [5](#)
- [36] A. Nan, M. Tennant, U. Rubin, and N. Ray, “Ordinary differential equation and complex matrix exponential for multi-resolution image registration,” arXiv preprint arXiv:2007.13683, 2020. [5](#)
- [37] S.-C. Pei, W.-L. Hsue, and J.-J. Ding, “Discrete fractional fourier transform based on new nearly tridiagonal commuting matrices,” IEEE Transactions on Signal Processing, vol. 54, no. 10, pp. 3815–3828, 2006. [6](#)
- [38] Z. Chen, A. Luo, and X. Huang, “Euler’s formula-based stability analysis for wideband harmonic resonances,” IEEE Transactions on Industrial Electronics, vol. 67, no. 11, pp. 9405–9417, 2019. [6](#)
- [39] J. Bruna, W. Zaremba, A. Szlam, and Y. LeCun, “Spectral networks and locally connected networks on graphs,” in Proceedings of the 2nd International Conference on Learning Representations, 2014. [7](#)
- [40] A. Bojchevski and S. Günnemann, “Deep gaussian embedding of graphs: Unsupervised inductive learning via ranking,” in Proceedings of the 5nd International Conference on Learning Representations, 2017. [9](#)
- [41] P. Sen, G. Namata, M. Bilgic, L. Getoor, B. Galligher, and T. Eliassirad, “Collective classification in network data,” AI magazine, vol. 29, no. 3, pp. 93–93, 2008. [9](#)
- [42] C. L. Giles, K. D. Bollacker, and S. Lawrence, “Citeseer: An automatic citation indexing system,” in Proceedings of the third ACM conference on Digital libraries, 1998, pp. 89–98. [9](#)
- [43] A. Bojchevski and S. Günnemann, “Certifiable robustness to graph perturbations,” in Advances in Neural Information Processing Systems, vol. 32, 2019. [9](#)
- [44] A. Bojchevski and S. Günnemann, “Adversarial attacks on node embeddings via graph poisoning,” in International Conference on Machine Learning. PMLR, 2019, pp. 695–704. [9](#)
- [45] W. Jin, Y. Ma, X. Liu, X. Tang, S. Wang, and J. Tang, “Graph structure learning for robust graph neural networks,” in Proceedings of the 26th ACM SIGKDD International Conference on Knowledge Discovery & Data Mining, 2020, pp. 66–74. [9](#)
- [46] L. Wang, Y. Zhang, and J. Feng, “On the euclidean distance of images,” IEEE transactions on pattern analysis and machine intelligence, vol. 27, no. 8, pp. 1334–1339, 2005. [11](#)
- [47] D. Zügner and S. Günnemann, “Adversarial attacks on graph neural networks via meta learning,” in Proceedings of the 6th International Conference on Learning Representations, 2018. [12](#)
- [48] A. Liu, Y. Wang, and T. Li, “Sfe-gacn: A novel unknown attack detection under insufficient data via intra categories generation in embedding space,” Computers & Security, p. 102262, 2021. [11](#)